PRAMANA
— journal of
physics

Vol. 41, No. 4,
October 1993
pp. 389–399

Dynamics of immiscible radial viscous fingering: A numerical study

SUBIR K SARKAR and DAVID JASNOW*
School of Physical Sciences, Jawaharlal Nehru University, New Delhi 110 067, India
*Department of Physics and Astronomy, University of Pittsburgh, Pittsburgh, PA 15260, USA

MS received 17 May 1993; revised 12 August 1993

Abstract. In this paper we undertake a numerical investigation of the dynamics of the interface in the problem of immiscible radial viscous fingering in a Hele–Shaw cell when the areal flow rate is maintained constant. Comparison is made with experimental results to check if there is a need to introduce velocity-dependent boundary conditions and to incorporate the effect of thickness of the film left behind by the moving interface. Some new scaling results are suggested by the numerical data. These data, along with those available from laboratory experiments, provide support for a mean field theory for radial immiscible viscous fingering published recently [*Phys. Rev. Lett.* **65**, 2680 (1990)].

Keywords. Viscous fingering; Fractals; Hele–Shaw flow.

PACS Nos 47·10; 68·10; 47·20; 81·30

1. Introduction

Viscous fingering in Hele–Shaw cells has served as a prototype of nonlocal interfacial pattern formation in systems far from equilibrium [1–6]. An important reason for this is that the equations of motion and the boundary conditions governing the dynamics of the interface as well as the conditions under which they are valid are known without any substantial ambiguity [3, 6]. The material parameters of the problem can be determined very accurately. Not all of these statements are applicable to the other two problems that have been studied rather extensively, namely free dendritic growth and directional solidification [7–9]. For this reason viscous fingering affords us an ideal system for quantitative tests of the various theoretical ideas that have been proposed. In particular, in the context of steady state pattern selection, it has provided a rather convenient testing ground for an accurate verification of the scenario of 'microscopic solvability' as the underlying mechanism [10, 11]. In contrast to the case of the rectangular geometry, much less progress has been made for fingering phenomena in the radial geometry [4, 5]. Here the steady state phenomena are replaced, in the simplest case, by a tip splitting cascade—leading to the generation of fractals; the problem is to understand the relationship between the structure and the dynamics [12, 13]. This problem has a lot of formal similarity with the diffusion-limited-aggregation (DLA) model proposed by Witten and Sander [14–16]. However, this relationship breaks down if the two fluids involved in the displacement process are immiscible. This is precisely the regime that we are interested in. Carefully controlled experiments on immiscible radial viscous fingering phenomena have been

performed [5] and the present work is an effort to complement and analyze the experimental data.

The goals of the present work are: (i) To study the dynamics on a computer and in the process satisfy ourselves that the dynamical equations employed do indeed provide a complete description of the observed data. In particular we have in mind whether velocity-dependent boundary conditions and allowing for finite film thickness are crucial [6, 10, 11]. This is important since any analytical work will be based upon these equations, and it is essential to establish their adequacy. (ii) To collect data that are not available from the experiments and (iii) to discover possible new aspects of the problem with special reference to scaling properties. Part (i) is qualitative to some extent since one can only detect qualitative deviations from those laboratory data which are not characterized in a precise quantitative manner. The organization of this paper is as follows: In § 2 we review the equations of motion of the interface. The field equations as well as the boundary integral version are given. Section 3 describes the numerical results in detail and § 4 contains the conclusions of this work. Here we should note that extensions have been made on the code used here to generate data on the domain of growth substantially beyond what is reported here. It seems that there is a crossover in some scaling properties as one goes beyond the 'intermediate' domain that we deal with here [17]. In this paper we limit ourselves to the task of presenting the numerical data in this intermediate time domain. This and ref. [5] provide the basis for a mean field theory of scaling in immiscible radial viscous fingering—a summary of which has already been published [13].

2. Equations of motion

In a radial Hele–Shaw viscous fingering experiment a fluid of lower viscosity drives out a liquid of higher viscosity—the first fluid being injected at the center of the cell. The cell is made up of a pair of thick and transparent circular plates, one placed on top of the other with a small gap. The plates are very smooth and the placement must be such that the spacing between the plates is constant to a very high degree (1% or better). For reasons to be explained below, we shall deal with a situation in which the displacing fluid is a gas. Also we choose the displaced liquid to be one that wets the cell. The experiment can be most simply performed under two kinds of operating conditions: (1) The displacing fluid is injected at a constant pressure and (2) the areal rate of the displacement of the liquid is constant. As in ref. [5] we choose the second condition since it offers some very definite advantages which will be noted below. Figure 1 is a schematic representation of the experimental arrangement to which the following equations refer.

The relationship between the fluid velocity $\mathbf{u}$, averaged over the direction transverse to the plates, and the pressure field (which does not vary in the transverse direction) is given by:

$$\mathbf{u} = -(b^2/12\mu)\nabla p \tag{1}$$

Here p is the pressure in the fluid and is a function of the x and y coordinates, the axes being in the plane of the plates; μ is the viscosity of the fluid and b is the spacing between the plates. Since we choose the displacing fluid to be a gas, μ is very small and it follows from (1) that the pressure is uniform within the gas, although it could be a function of time. Next, since the displaced liquid is incompressible, $\nabla \cdot \mathbf{u} = 0$,

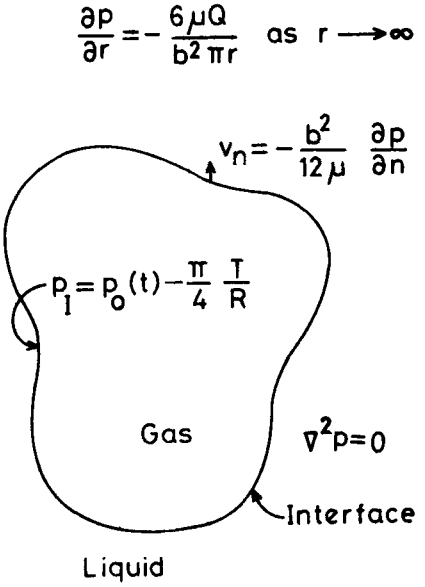

Figure 1. Schematic diagram of the experimental arrangement and the equations of motion.

which leads to the field equation for the pressure:

$$\nabla^2 p = 0. \tag{2}$$

During the motion of the interface, the liquid is not completely displaced by the gas even if the liquid wets the cell. For values of the normal velocity of the interface not too large, the thickness (t) of the liquid layer left behind on each of the plates is given by

$$t = 0{\cdot}67b(\mu v_n/T)^{2/3}. \tag{3}$$

v_n,the normal velocity of the interface, is related to the normal velocity (u_n) of the liquid immediately ahead by

$$u_n = v_n(1 - 2t/b). \tag{4}$$

Equation (1) gives the instantaneous normal velocity of the interface once the pressure field is determined. But for this one needs to know the boundary conditions in addition to the field equation (2). The far field boundary condition is determined from the fact that the velocity field is radially outward and is independent of the angular position. Combining this with the fact that the flux is constant, one can determine the pressure gradient from (1). Hence at large distances

$$dp/dr = -(6\mu Q/b^2\pi r), \tag{5}$$

where Q is the areal displacement rate. On the liquid side of the interface, the pressure (p_l) is given by the Park–Homsy equation [6]:

$$p_l = p_0(t) - [(\pi T/4R) + 7{\cdot}6(T/b)(\mu v_n/T)^{2/3}]. \tag{6}$$

This equation is valid when ($\mu v_n/T$) is much less than unity and the liquid wets the

cell. Here $p_0(t)$ is the uniform pressure within the gas, R is the radius of curvature of the interface in the plane of the plates and T is the surface tension between the two fluids. Unfortunately, in (3), (4) and (6) one has to deal with nonlinear terms which would make numerical computation of the dynamics even more extensive. For this reason, we assume that the velocity-dependent terms in the boundary condition and the finiteness of the film left behind can be ignored; in this work we have set $t=0$ and $u_n = v_n$. In the constant-flux operating mode the maximum interfacial velocity decreases as the structure grows so that the velocity-dependent correction decreases in absolute terms. But given the fact that the deviation from the constant pressure condition on the interface is small anyway compared to the viscous pressure drop and that small terms are known to affect long-term dynamics in these problems, one cannot be sure, a priori, about the validity of this approximation. In fact, by way of comparison with experimental data, we want to check that ignoring the velocity-dependent correction does not at least introduce qualitative changes. One more advantage of having constant flux and ignoring velocity-dependent terms as well as film thickness is that the dynamics can be made entirely dimensionless by choosing appropriate units for pressure, length and time [18]. So the description becomes completely independent of material parameters and is thus applicable to any liquid-gas pair.

Since we are interested in the dynamics of the interface and not in the pressure field everywhere, a convenient way to do the numerical calculation is provided by an equation which involves only the interfacial degrees of freedom. In the dimensionless units mentioned above, this equation is [19]:

$$-(1/2R(s)) = \int_{\text{Interface}} [G(s,s')v_n(s') - (1/R(s'))\nabla' G \cdot \mathbf{n}(s')]\,ds' + C_0(t). \quad (7)$$

The dynamics are described in terms of a function $\Theta(s)$ which is the tangent angle as a function of the arclength parameter (s). G is the Green's function given by $G(s, s') = -(1/2\pi)\ln|\mathbf{r}(s) - \mathbf{r}(s')|$, $\mathbf{r}(s)$ being the two-dimensional position vector for the interfacial point with the arclength coordinate s. $C_0(t)$ depends on time only and is found as a part of the solution. $\mathbf{n}(s')$ is the unit normal vector directed into the displaced fluid at the point s'. The flux conservation equation is given by

$$\int_{\text{Interface}} v_n(s)\,ds = 2\pi \quad (8)$$

The constant $C_0(t)$ has its origin in the boundary condition on the pressure field at infinity and its instantaneous value can be determined by combining (7) and (8). Once the normal velocities are found from (7) and (8), the change in the interface follows from geometrical considerations. The time evolution of $\Theta(s)$ is calculated from the equation

$$d\Theta(\alpha)/dt = -(1/S_T)(\partial v_n/\partial\alpha) - (S_T/R(\alpha))[g(\alpha) - \alpha g(1)], \quad (9)$$

where $\alpha = s/S_T$, S_T being the instantaneous total length of the interface. Thus $0 \leqq s \leqq S_T$. $g(\alpha)$ is defined by

$$g(\alpha) = \int_0^\alpha [v_n(\alpha')/R(\alpha')]\,d\alpha'. \quad (10)$$

The time dependence of S_T is given by

$$dS_T/dt = S_T g(1). \tag{11}$$

A numerical scheme for solving this type of integro-differential equations has been described elsewhere [19].

3. Results

Before comparing the numerical results directly with the experimental data, it is important to remember certain aspects of the code we use. For a sinusoidal perturbation of m-fold symmetry, the initially circular interface becomes unstable when the radius of the circle exceeds some critical value r_m. In an experiment the initial deformation is typically of five bulges, but they are certainly not fully symmetric. The source of this perturbation presumably is the nonuniformity of the spacing between the plates (which is always present and cannot be controlled beyond a certain limit). In the numerical scheme there is no such noise except for what is inherent to any such code and in the initial deformation of the interface with four-fold symmetry. Ideally one would like to start with a radius near r_4. Unfortunately we have to take an initial radius several times this value. The reason being that the interface is discretized into N_G points equally spaced in arclength. In order to maintain a proper level of resolution N_G is dynamically increased as the structure grows. However, for a given choice of the dimensionless growth step ε (defined as the maximum value of the ratio of the local normal interface displacement to the local radius of curvature in one step of integration) and for a given value of S_T, N_G cannot be increased beyond a limit without introducing numerical instabilities. At the same time, if the value of N_G is lower than about 100 (even for a near circular interface) the resolution is unacceptable. The only way to satisfy all these constraints is to start with a radius which is substantially higher than r_4. We always start with a total arclength of 1900 and a small four-fold symmetric perturbation so that $\Theta(\alpha)$ is of the form

$$\Theta(\alpha) = 2\pi\alpha + \beta \sin(8\pi\alpha), \tag{12}$$

with $\beta = 0{\cdot}05$. But, as we have mentioned already, the radius is much higher than r_4 so that we are starting with a small perturbation in a domain where the interface is well into the region of instability. Clearly, this fails to mimic the 'real life' growth at early times. However, at later times this may become immaterial. In particular, we hope that it does not influence the scaling aspects of the dynamics. Our final remark is concerned with the numerical detection of the existence of scaling itself. A basic criterion for this is that the data should span a sufficiently wide range of scales. In our simulations the range of the data available before numerical errors become unacceptable is essentially the same as in with the data the laboratory setup of ref. [5]. For some pairs of variables this range provides convincing evidence of scaling. But for some others it is not so satisfactory and our search for scaling has been guided partially by the mean field theory that has been developed [13].

3.1 *Fractal geometry and fractal dimension*

Sander *et al* [20] have also performed numerical integration on the same problem, but with the difference that in their work the pressure was maintained constant inside the driving fluid. In contrast we maintain a constant flux condition. Except for the

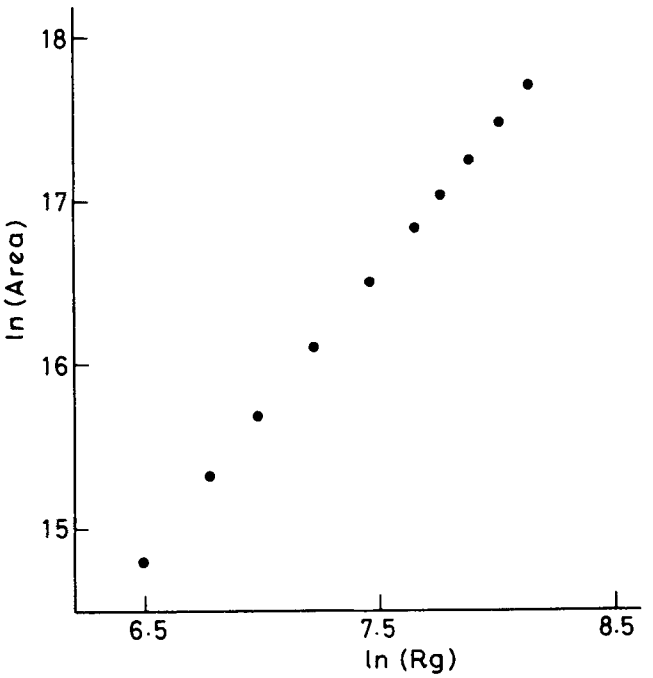

Figure 2. Area vs radius of gyration in one run. The slope is d_f.

artificial four-fold symmetry we impose, there is no qualitative distinction between the time evolution of the interface in the laboratory and in the numerical experiments. The fractal nature of the structure is reflected in figure 2 from which the fractal dimension d_f is measured to be 1·77. The experimental value for d_f obtained by May and Maher [5] is $1{\cdot}79 \pm 0{\cdot}04$.

3.2 *Radius of gyration R_g vs radius of structure R*

In the context of radial viscous fingering in porous media, it is known [21] that the radius of gyration is proportional to the radius of the structure (the distance between the center of the structure defined as the point where the growth started and the point of the structure farthest from the centre)–with the constant of proportionality $h = R/R_g$ equal to $1{\cdot}98 \pm 0{\cdot}03$. Data on this aspect have not been reported in ref.[5]. Our numerical data (figure 3) demonstrate that for the present problem also, the proportionality is satisfied very well but with a rather different value of h. Here $h = 1{\cdot}53$. This lower value of h is due to the fact that in the present case the tips have the shape of pies that increase in width in the radially outward direction, and thus the parts of the structure which are further away from the centre receive a higher weighting in the radius of gyration as compared with the case of fingering in porous media. There the structure is very stringy and the width of the branches are only very weakly dependent on the distance from the centre. Thus for a given value of the radius of the structure, the radius of gyration would be expected to be larger in the case of immiscible radial viscous fingering than in the case of fingering in porous media. By the same argument, the value of h for the standard DLA model of Witten and Sander [14] should also be higher than the value for our present problem. One of the physical quantities defined by Rauseo *et al* [5] is the area of mixing (A_{mix}) which is equal to $\pi(r_{max}^2 - r_{min}^2)$ where r_{max} and r_{min} are the maximum and minimum

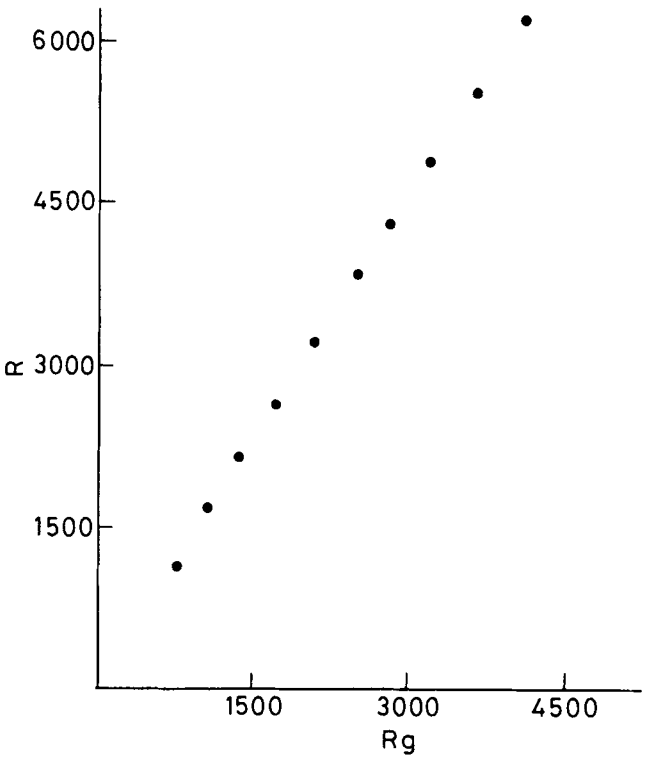

Figure 3. Radius of the structure vs. radius of gyration.

values of the radial coordinate over all the points of the interface. Thus r_{max} is nothing but the radius of the structure. r_{min} corresponds to some point deep in the interior, and since the growth is essentially absent in such shielded regions, r_{min} changes little during the growth and very soon r_{max}^2 dominates. Thus A_{mix} is essentially equal to πR^2 and is equivalent to the radius of the structure (R) from the point of view of scaling properties. For this reason we do not separately analyze A_{mix} in this paper.

3.3 *Total arclength (S_T) of the interface*

In the classical 2-*d* DLA problem on a square lattice, one can define the arclength as the number of interfacial points. Here the interfacial points are those points of the aggregate which have at least one empty neighboring point. But since the probablity of having all the four neighbouring lattice points occupied is rather small, the length of the interface as defined above is essentially the same as the mass of the aggregate. One encounters a similar problem of definition for radial miscible viscous fingering [16] or for fingering in porous media [21]. In the present problem these difficulties are absent, and the total arclength is an interesting and independent parameter to study. Reference [5] also defines a reduced quantity called the stretching parameter $\varphi = [(S_T/2\pi\sqrt{2R_g}) - 1]$. Obviously its scaling properties are not independent of those of S_T which is what we will limit our attention to here. However, to obtain a qualitative comparison with the data of ref.[5], we present our numerical results on the stretching parameter along with the laboratory data in figure 4. To uncover possible new scaling relations, $\ln(S_T)$ is plotted as a function of ln(area) in figure 5a. The experimental data displayed in figure 5b combines data from several

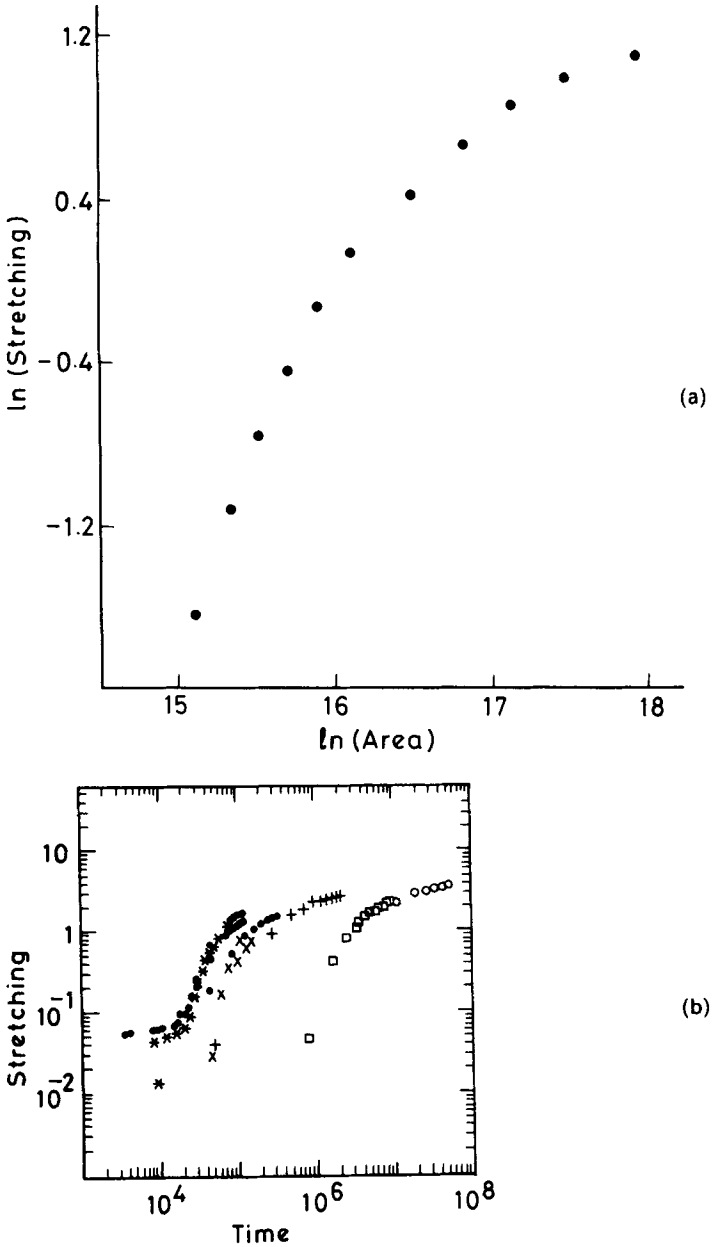

Figure 4. (a) Stretching vs area for a typical run in the numerical experiment. (b) Log–log plot of stretching vs area from laboratory experiment (ref. 5). Different symbols are used for data for different runs which have different areal flow rates and/or plate spacings. Since the areal flow rate in dimensionless units is always equal to 2π, time is equivalent to area.

runs with different values of flow rates and/or gap width of the Hele-Shaw cell. If we use the data from our numerical calculation or from a single run in figure 5b (to which the numerical data corresponds), the value of the scaling index thus obtained would be too uncertain. For this reason we have used the data of figure 5b which spans a much wider range and helps us obtain a much less uncertain value of the

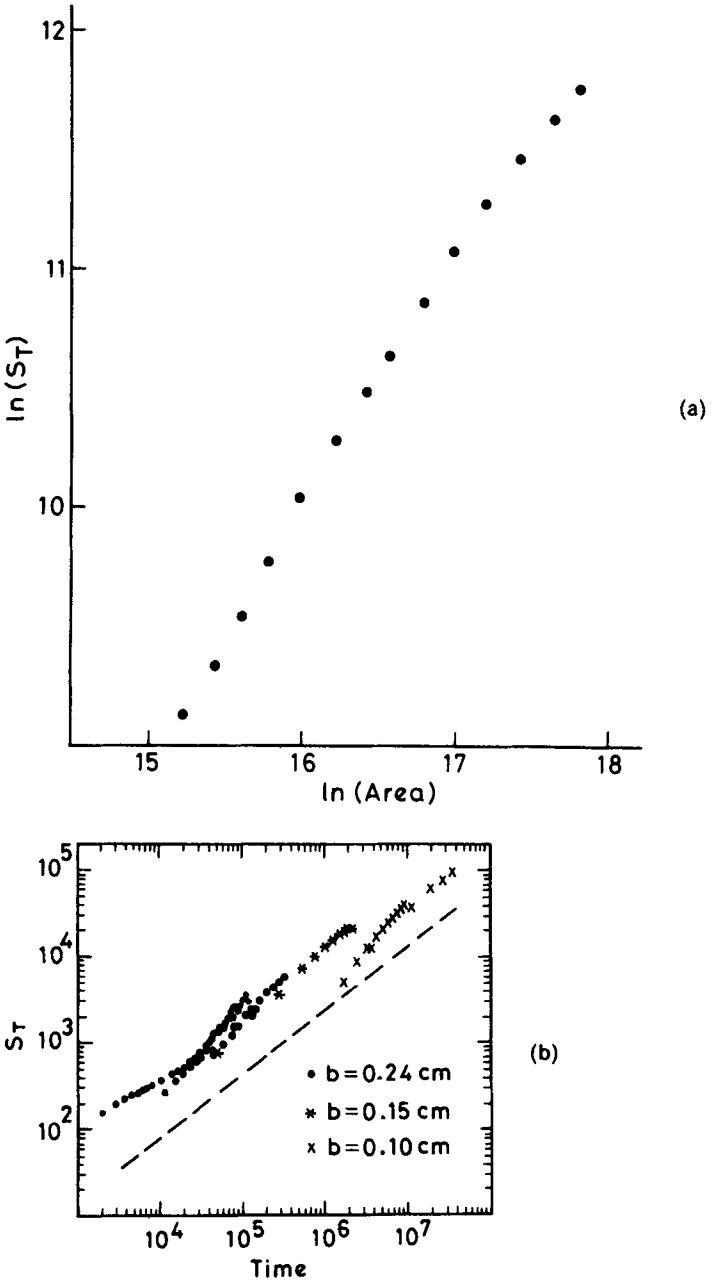

Figure 5. (a) Total arclength vs area. (b) Total arclength vs area from laboratory data (ref. 5). Different symbols are for different runs. Time is equivalent to area.

scaling index d_{SA}—defined here as the slope of $\ln(S_T)$ vs ln(area). The estimate for d_{SA} is 0·74 (calculated on the basis of the dashed straight line in figure 5b). The assumption made here implicitly is that the total arclength is proportional to (area)^z where $z = d_{SA}$ and the constant of proportionality depends on the area at the most in a rather weak manner. If this constant of proportionality is different for different runs, then this determination of d_{SA} by combining data from different runs is no more reliable than what would be the case if we tried to evaluate it from a single

run. The assumption that we have made is trivially true for a growing circle and is also consistent with the data in figure 5b.

We note here that a recent work [22] also provides data on this although the boundary conditions are rather different. Translated to our problem, this work presents numerical data on a flow in which the pressure is maintained constant at a higher value inside the gas and at a lower value on a circle of large radius. A log-log plot of ($S_T/\sqrt{\text{area}}$) as a function of S_T is presented. The linearity of the curve is convincing and we read off the slope to be approximately 0·35. The value of 0·74 for d_{SA}, as obtained from figure 5b, would imply a value of 0·324 for this slope. However, one has to carefully analyze the implications of the difference of boundary conditions to see whether they should influence the scaling properties. If one can demonstrate that the scaling, at least for this pair of variables, should be identical for these two different kinds of boundary conditions then this work supports the present one.

4. Conclusions

We have not seen any qualitative difference between the experimental data and our numerical results using a model that excludes the velocity-dependent part of the boundary condition and the effect of finite film thickness. Of course this, by itself, does not ensure that these factors can be ignored for all purposes. But our conclusion is further supported by the excellent agreement between the laboratory and the numerical data for the value of the fractal dimension. The numerics also provide a very precise value for the ratio between the radius of the structure and the radius of gyration. Unfortunately this ratio is not available for the laboratory experiments.

To summarize, these results lead us to believe that a model with just the surface tension in the boundary condition should be adequate for a theoretical description of the radial immiscible viscous fingering experiments of ref. [5]. It is significant that there was no need to incorporate noise explicitly to trigger tip-splitting. The results for the scaling of the total length of the interface as a function of the radius of gyration are new and have found theoretical support [13]. The mean field analysis of ref. [13] also predicts that scaling in this problem is subject to a periodic modulation. Thus if x and y are the scaling variables of interest, then if $\ln(x)$ is plotted as a function of $\ln(y)$, one should obtain a periodically modulated straight line. The amplitude of modulation depends on the particular pair of variables concerned. In such a curve, a segment spanning only about one period will indeed look like the data for a single run from both the numerical and the laboratory experiments as has been reported in this paper. Also the amplitude of modulation will determine the degree of uncertainty of the estimated value of the slope of the underlying straight line if one has such limited data. Finally, it should be noted that we have avoided quoting estimates of error bars on the various scaling amplitudes or exponents. As should be obvious from the context, none of the standard techniques of estimation of error bars work in the present case. The way to do is to generate the data on the interface dynamics for many different initial conditions, estimate exponents or amplitudes the way it has been done here and then to perform statistical analysis in order to estimate the error bars. Obviously, this error bar would be a measure of the sensitivity of the scaling aspects with respect to the initial conditions.

Acknowledgements

The authors wish to thank the Pittsburgh Supercomputer Centre for providing the computing facilities needed for this work. Part of the financial support was provided by the National Science Foundation. The authors also thank James V. Maher and Mark DiFrancisco for many useful discussions on the various aspects of the experiment.

References

[1] J S Langer, *Rev. Mod. Phys.* **52**, 1 (1980)
[2] P Pelcé: *Dynamics of curved fronts* (Perspectives in Physics series), edited by H Araki, A Libchaber and G Parisi (Academic Press, New York, 1988)
[3] D Bensimon, L P Kadanoff, S Liang, B I Shraiman, and C Tang, *Rev. Mod. Phys.* **58**, 977 (1986)
D A Kessler, J Koplik and H Levine, *Adv. Phys.* **37**, 255 (1988)
[4] J Bataille, *Rev. Inst. Pétrole* **23**, 1349 (1968)
L Paterson, *J. Fluid Mech.* **113**, 513 (1981)
[5] S N Rauseo, P D Barnes, and J V Maher, *Phys. Rev.* **A35**, 1245 (1987)
S E May and J V Maher, *Phys. Rev.* **A40**, 1723 (1989)
[6] C W Park and G M Homsy, *J. Fluid Mech.* **139**, 291 (1984)
[7] S C Huang and M E Glicksman, *Acta Metall.* **29**, 701, 717 (1981)
[8] K Somboonsuk, J T Mason and R Trivedi, *Metall. Trans.* **A15**, 967 (1984)
R Trivedi, *Metall. Trans.* **A15**, 977 (1984)
[9] S de Cheveigné, C Guthmann, and M M Lebrun, *J. Phys. (Paris)* **47**, 2095 (1986)
[10] P G Saffman and G I Taylor, *Proc. R. Soc. London, Ser.* **A245**, 312 (1958)
P Tabeling and A Libchaber, *Phys. Rev.* **A33**, 794 (1986)
P Tabeling, G Zocchi, and A Libchaber, *J. Fluid Mech.* **177**, 67 (1987)
[11] S K Sarkar and D Jasnow, *Phys. Rev.* **A35**, 4900 (1987) and references therein.
[12] H Thomé, M Rabaud, V Hakim and Y Couder, *Phys. Fluids* **A1**, 224 (1989)
M Ben-Amar, *Phys. Rev.* **A43**, 5724 (1991)
[13] S K Sarkar *Phys. Rev. Lett.* **65**, 2680 (1990)
[14] T A Witten and L M Sander, *Phys. Rev. Lett.* **47**, 1400 (1981)
[15] L Paterson, *Phys. Fluids* **28**, 26 (1985)
[16] G Daccord, J Nittmann and H E Stanley, *Phys. Rev. Lett.* **56**, 336 (1986)
[17] D Jasnow and C Yeung, *Phys. Rev.* **E47** 1087 (1993)
[18] S K Sarkar, *Superlattices and microstructures* **3**, 589 (1987)
[19] S K Sarkar and D Jasnow, *Phys. Rev.* **A39**, 5299 (1989)
[20] L M Sander, P Ramanlal and E Ben-Jacob, *Phys. Rev.* **A32**, 3160 (1985)
[21] K J Måløy, F Boger, J Feder and T Jøssang, *in Time dependent effects in disordered materials*, edited by R Pynn and T Riste (Plenum, New York, 1987)
[22] T H Tɔng and J A O'Brien, *Phys. Rev.* **A41**, 4430 (1990)